

Study of intra-particle diffusion effect on hydrodesulphurization of dibenzothiophenic compounds

Jinwen Chen^{*}, Hong Yang, Zbigniew Ring

National Centre for Upgrading Technology (NCUT), One Oil Patch Drive, Devon, Alta., Canada T9G 1A8

Available online 3 October 2005

Abstract

In this paper, the intra-particle diffusion effect on hydrodesulphurization of dibenzothiophenic compounds in light cycle oil was experimentally studied. The catalyst effectiveness factors were determined with a full-size commercial NiMo/Al₂O₃ hydrotreating catalyst and its crushed catalyst particles under similar operating conditions. In the full-size commercial catalyst, significant intra-particle diffusion resistance was present, resulting in reduced sulphur removal reaction rates for all the dibenzothiophenic compounds investigated. The effectiveness factors ranged from only 0.300 to 0.822 in the temperature range of commercial importance. In the crushed catalyst, the intra-particle diffusion limitation was mostly eliminated with the corresponding effectiveness factors between 0.813 and 0.985. The DBTs with little or no steric hindrance effect, and thus with high intrinsic reactivities, had lower effectiveness factors, indicating a stronger intra-particle diffusion resistance. Those with strong steric hindrance effect, and thus with low intrinsic reactivities, had higher effectiveness factors, showing a weaker intra-particle diffusion limitation. Crown Copyright © 2005 Published by Elsevier B.V. All rights reserved.

Keywords: Hydrodesulphurization; Dibenzothiophenic compounds; Intra-particle diffusion

1. Introduction

In the near future, environmental regulations in most developed countries will require significant reductions of sulphur and nitrogen contents in diesel and other transportation fuels in order to further reduce SO_x and NO_x pollution caused by engine exhaust emissions [1,2]. This challenging task calls for collaborating efforts among refineries, catalyst manufacturers, technology developers and R&D organizations. Although, in recently years, some alternative technologies have been studied and developed [3,4], particularly to reach new stringent sulphur specifications in finishing fuel blending stocks, hydrotreating that involves hydrodesulphurization (HDS) and hydrodenitrogenation (HDN) is and will remain the dominant refining technology to remove sulphur and nitrogen from petroleum fractions [1].

During hydrotreating of middle distillates and heavier petroleum feedstocks, trickle-bed reactors are commonly used in which HDS and HDN reactions are carried out on catalyst surface under high temperatures and pressures. In a commercial

trickle-bed hydrotreating reactor, catalyst particles with diameters of 1.3–3.2 mm and average lengths of 5–10 mm are commonly used. This range of catalyst sizes reflects the tradeoff between the desire to provide high catalyst utilization (high catalyst effectiveness factors) on one hand, and to maintain a manageable pressure drop across the reactor on the other. Within this range of catalyst particle size, the intra-particle diffusion resistance (the diffusion of sulphur compounds inside the catalyst pores) could significantly reduce the overall HDS reaction rate. Furthermore, the intra-particle diffusion effect varies with operating conditions (particularly with temperature) and sulphur compounds of different intrinsic reactivities. While this issue is very important for a full understanding of HDS mechanisms and processes, it has not been adequately and quantitatively addressed in the open HDS literature, although many HDS studies have been conducted separately with either full-size catalysts [5–8] or crushed catalyst particles [9,10].

This study focuses on the experimental determination of the effectiveness factors of different dibenzothiophenic compounds (DBTs) that are commonly found in cracked light distillates. The study is one of the hydroprocessing model development activities being conducted at the National Centre for Upgrading Technology (NCUT), and serves here as a reminder of the

^{*} Corresponding author. Tel.: +1 780 987 8763; fax: +1 780 987 5349.

E-mail address: jjchen@NRCan.gc.ca (J. Chen).

important effect of physical and transport phenomena on hydrodesulphurization rates. These phenomena, including intra-particle diffusion (dealt with in this paper) and vapor–liquid phase equilibrium in the reactor [11,12] are usually ignored in the very large number of papers dealing with kinetics analysis of HDS reactions, and even in most commercial hydroprocessing models.

2. Experimental

This experimental program was performed in a pilot plant hydrotreating unit. A detailed description of the experimental set-up, procedures, and analytical methods have been provided elsewhere [5,6]. Only a brief summary of the experimental program is given below.

The experimental set-up, shown in Fig. 1, was a bench-scale reactor system consisting of a single reactor, a high-pressure phase separator and a product stabilizer. Gas flowed once through the system without recycling. The reactor was configured to simulate a commercial single-stage hydrotreater under operating conditions of industrial interest, and was operated in co-current down-flow (trickle-flow) mode. The hydrotreating reactor, a stainless steel tube of 1 m long and 2.54 cm in diameter (i.d.), was equipped with a 0.64 cm (o.d.) centrally located thermowell that housed 12 thermocouples for detailed measurement of the axial temperature profile in the reactor. Two sets of hydrotreating experiments were conducted. In the first one, the reactor was packed with 140 ml of full-size commercial NiMo/Al₂O₃ hydrotreating catalyst (extrudates of 1.6 mm in diameter and, on average, 5 mm in length). This catalyst was diluted with 0.2 mm glass beads in the 1:1 volumetric ratio. The total catalyst bed height was 57 cm. In the

second set of experiments, the reactor was packed with 118 ml of 35–60 mesh (0.25–0.5 mm) catalyst particles obtained by crushing the full-size commercial NiMo/Al₂O₃ hydrotreating catalyst. No glass beads were used to dilute the catalyst bed. The bed height in the second set of experiments was 24 cm.

Both sets of experiments were conducted with co-current down-flow of gas and liquid in the trickle-flow regime. Prior to the hydrotreating experiments, the fresh catalysts (both the full catalyst and the crushed one) were sulphided and stabilized by processing the same cracked feedstock, light cycle oil (LCO), from a fluid catalytic cracking unit for about 500 h under operating conditions similar to those used in the experiments. A flat axial temperature profile was maintained throughout the program. The feedstock and products were analyzed for C and H, simulated distillation (SimDis), and density using standard ASTM methods. These analytical data, together with the process data acquired (i.e. the feed, product, hydrogen and vent gas rates, vent gas composition, etc.), were subsequently used to perform detailed carbon, hydrogen and overall mass balance calculations. At each set of operating conditions at steady state, the liquid product was gathered during two 3 h back-to-back mass balance periods. Since it was shown that these kinds of experiments have routinely generated repeatable results [6], to reduce the related analytical work, a sample of only one liquid product was analysed in detail at most of the conditions. The other sample was analyzed only when unexpected results were observed.

The key physical properties of the feed LCOs used in the two sets of experiments are listed in Table 1. All the physical properties of the two feeds are quite close to each other.

Total nitrogen and sulphur in the feed and hydrotreated effluents were analyzed with a DOHRMAN-chemiluminescence instrument (ASTM D4629) and a gas chromatograph

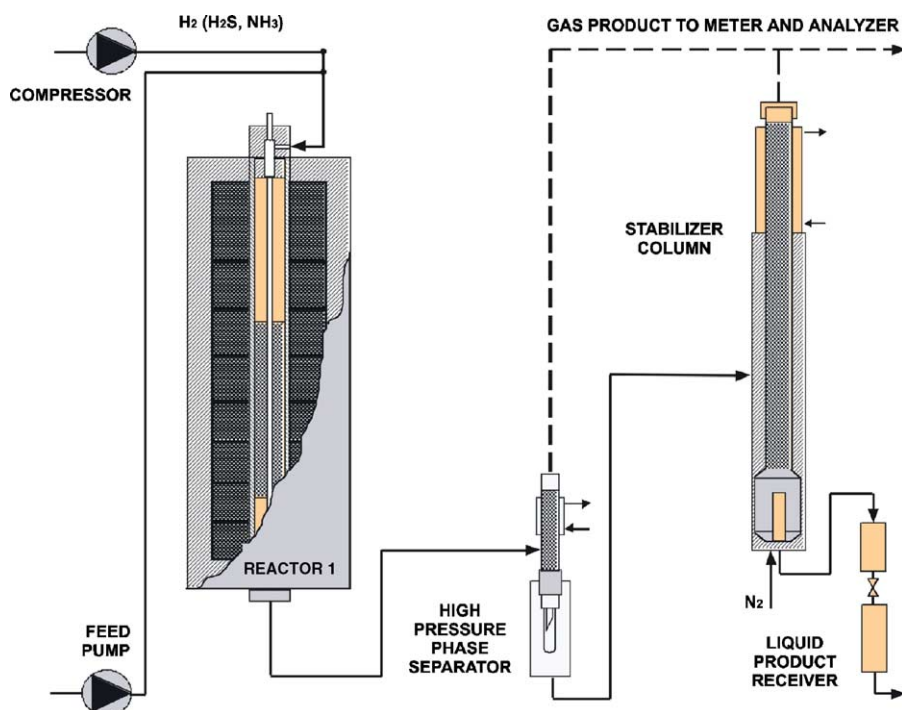


Fig. 1. Diagram of the Pilot Plant Hydrotreating Unit.

Table 1
Composition and physical properties of the LCO feeds

	Feed 1 (used for full-size catalyst)	Feed 2 (used for crushed catalyst)
Density (15 °C) (g/ml)	0.960	0.936
Carbon (wt.%)	89.13	88.20
Hydrogen (wt.%)	9.84	10.84
Total sulphur (wppm)	8686.2	7072.8
Total nitrogen (wppm)	730.9	660.7
Aromatics (wt.%)	83.76	71.27
Paraffins (wt.%)	6.80	8.91
Cycloparaffins (wt.%)	8.87	19.82
SimDis (°C)		
IBP	113.8	128.4
10 wt.%	230.9	225
30 wt.%	258.8	255.3
50 wt.%	289.1	288.5
70 wt.%	328.7	326.4
90 wt.%	373.5	372.4
FBP	431.9	430.8

with a sulphur chemiluminescence detector (GC-SCD, ASTM D5623), respectively. The quantification of individual sulphur compounds in the feed and hydrotreated effluents was achieved with a gas chromatograph with an atomic emission detector (GC-AED, sulphur channel 181 nm) using the external-standard method. The identification of individual compounds, dibenzothiophenic compounds in this study, was achieved by matching the retention times of their corresponding peaks with those of standard compounds collected in the database of the National Centre for Upgrading Technology (NCUT). More details on sulphur speciation and quantification can be found elsewhere [5,6]. About 70 sulphur compounds could be positively identified in the LCO feed. This paper focuses on 25 of them, including dibenzothiophene (DBT) and its one-, two- or three-alkyl (methyl, ethyl) substituted derivatives.

This experimental study was conducted in the reaction temperature range of 350–400 °C and liquid space velocity range of 1.58–4.5 h⁻¹, while other conditions were fixed at the total pressure of 69.1 atm, gas-to-oil ratio of 1000 NL(gas)/kg(feed) and H₂S concentration in the treat gas of 0.5 vol%.

3. Results and discussions

3.1. Sulphur speciation

The sulphur chromatogram of the LCO feedstock used in this study is shown in Fig. 2. The individual peaks in the chromatogram mostly correspond to thiophenic (TH), benzothiophenic (BT), dibenzothiophenic (DBT)/naphthothiophenic (NTH) and benzo-naphthothiophenic (BNTH) compounds with various degrees of substitution of relatively short paraffinic chains at different positions. In general, the peaks with shorter retention times represent thiophenic and benzothiophenic compounds while those with longer retention times represent dibenzothiophenic/naphthothiophenic and benzo-naphthothiophenic compounds.

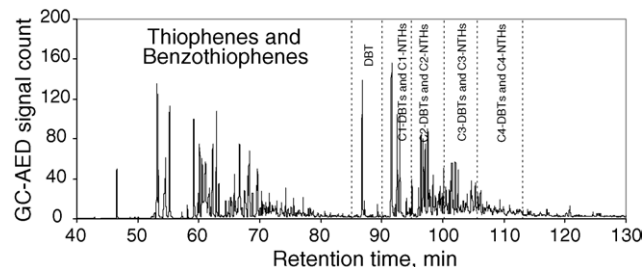


Fig. 2. Sulphur chromatogram of one of the LCO feeds.

Figs. 3 and 4 show the sulphur chromatograms of the hydrotreated products obtained at reactor temperature of 350 °C with the full-size and the crushed catalyst beds, respectively. A comparison of the feed and effluent chromatograms indicates that the thiophenic, benzothiophenic compounds, and even DBT were completely removed in both reactor effluents but alkyl-substituted DBTs and NTHs persisted. A comparison between Figs. 3 and 4 shows that under similar operating conditions not only more sulphur but also more sulphur compounds were removed over the crushed catalyst (Fig. 4) than over the full-size catalyst (Fig. 3) pointing to improved effectiveness of the crushed catalyst discussed in detail below.

3.2. HDS reaction kinetics

In this study, HDS experiments were performed at several temperatures ranging from 350 to 400 °C for both the full-size catalyst bed and the crushed catalyst bed. As reported in our previous studies [5,6], the total sulphur and nitrogen removal, as well as the removal of individual sulphur compounds were

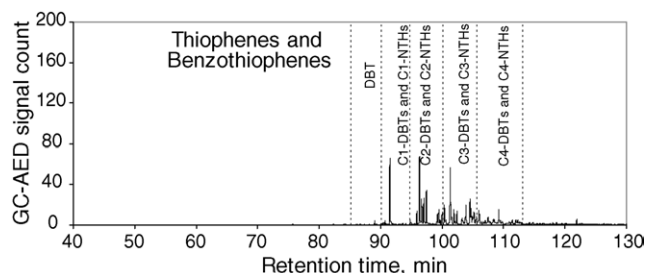


Fig. 3. Sulphur chromatogram of effluent at 350 °C, SV = 1.58 h⁻¹ (full-size catalyst).

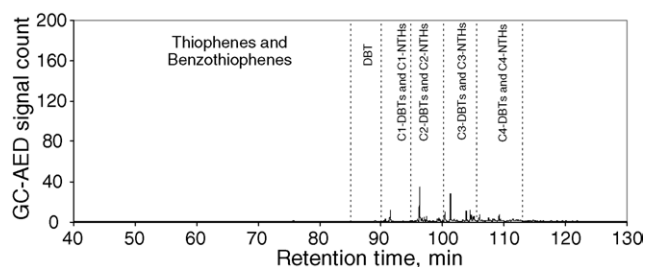


Fig. 4. Sulphur chromatogram of effluent at 350 °C, SV = 1.70 h⁻¹ (crushed catalyst).

well described by pseudo-first-order reaction kinetics up to 385 °C. At higher temperatures, the effect of hydrogenation/dehydrogenation equilibrium and the effect of vapor–liquid phase equilibrium became significant [12,13] and the pseudo-first-order kinetics were not applicable any more. In this case, more sophisticated kinetics models will have to be used in conjunction with detailed vapor–liquid phase equilibrium treatment. The work on modeling these data using actual liquid phase concentrations of individual sulphur compounds obtained from experiments for a separate study is currently underway and the results will be reported in the future.

It was assumed that for both full-size and crushed catalysts the reactor could be described by a plug-flow model, which is reasonable because of the small size of the crushed catalyst particles and the dilution with 0.2 mm glass beads in the full-size catalyst bed. Therefore, the pseudo-first-order reaction rate constant could be easily calculated from space velocity, and the measured sulphur concentrations in the feed and reactor effluent. Fig. 5 shows a typical Arrhenius plot of the pseudo-first-order reaction rate constants for 4-methyldibenzothiophene (4-MDBT) in the temperature range of 350–385 °C with both full-size and crushed catalysts. At the operating conditions used in this study, the straight lines fitting the experimental data points in the $\ln(k)$ versus $1/T$ coordinates indicate that the pseudo-first-order reaction assumption in this temperature range is reasonably good. At the same temperatures, the reaction rate constants obtained with the crushed catalyst is much higher than those obtained with the full-size catalyst. This is an indication that substantial intra-particle diffusion limitation was present in the full-size catalyst particles. All other dibenzothiophenic compounds investigated in this study, as well as the total sulphur removal, showed similar trends as those in Fig. 5.

It should be noted that many researchers have observed reaction orders greater than 1 (ranging from 1 to up to 4) for total sulphur removal with real petroleum feedstocks [7,8,14,15], attributable to the widely ranging reactivities of various sulphur compounds in the feed. This is especially true if the temperature range being investigated is relatively wide. Ancheyta et al. [15] have reviewed and compared some published apparent reaction orders for total sulphur removal obtained with different feedstocks. They concluded that the apparent reaction order for total sulphur removal increases with

the increase in molecular weight of the feed and the increase in total sulphur content in the feed [15].

3.3. Catalyst effectiveness factors

According to chemical reaction engineering fundamental theory, intra-particle diffusion becomes a limiting factor to the overall reaction rate when the catalyst particle size is too large and/or the intrinsic reaction rate is too fast compared to the diffusion rate of reacting molecules inside the catalyst pores. The degree of the resulting inhibition of the overall rate depends on the combination of particle size and shape, intrinsic reaction rate and diffusion rate. Since it was not certain that the crushed catalyst particles used in this study were small enough to completely eliminate intra-particle diffusion effect in the temperature range of 350–385 °C, it was assumed that this limitation was present in both catalysts at different degrees. We assumed that the performance of the cylindrical catalyst was well represented by the infinite cylinder geometry, and that of the crushed catalyst by the spherical geometry. As indicated in the previous section, in the range of conditions used, the kinetics of the reactions in question was close to pseudo-first-order. Therefore, the catalyst effectiveness factors for catalysts of both types were calculated according to the following equations:

$$k = \eta k_{\text{intrinsic}} \quad (1)$$

where

$$\eta = \frac{I_1(2\phi)}{\phi I_0(2\phi)} \quad (2)$$

(for cylinders of infinite length, full-size catalyst)

$$\eta = \frac{1}{\phi} \left(\frac{1}{\tanh(3\phi)} - \frac{1}{3\phi} \right) \quad (\text{for spheres, crushed catalyst}) \quad (3)$$

$$\phi = \frac{V_p}{S_p} \sqrt{\frac{k_{\text{intrinsic}}}{D_e}} \quad (4)$$

In the above equations, k and $k_{\text{intrinsic}}$ are the apparent and intrinsic pseudo-first-order reaction rate constants, η the catalyst effectiveness factor, ϕ the Thiele modulus, D_e the effective diffusivity inside the catalyst particle and V_p and S_p are the volume and surface area of the catalyst particle, respectively. By applying the above equations to both the full-size and the crushed catalyst data at the same temperature, $k_{\text{intrinsic}}$ and D_e were calculated for each individual sulphur compound. The catalyst effectiveness factor was then calculated from Eq. (1).

In this paper, the pseudo-first-order reaction rate constants at different temperatures were calculated for each individual sulphur compound according to its concentrations in the feed and hydrotreated effluent, and the space velocity used. In order to filter out experimental errors and reliably estimate the

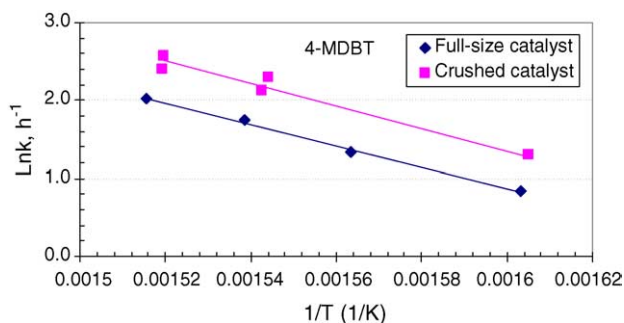


Fig. 5. Pseudo-first-order rate constants for 4-MDBT at different temperatures.

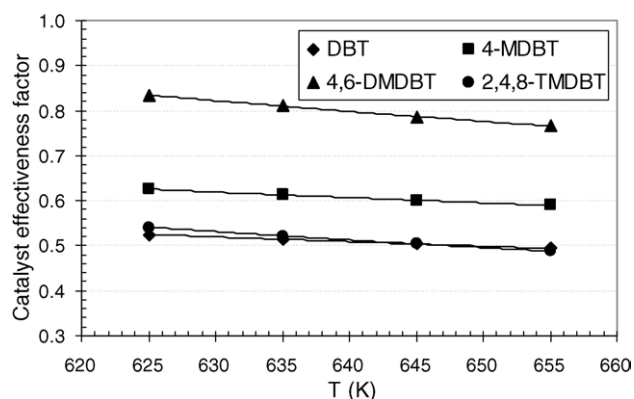


Fig. 6. Catalyst effectiveness factors for DBT, 4-MDBT, 4,6-DMDBT and 2,4,8-TMDBT at different temperatures.

individual effectiveness factors from the limited number of experimental points, the reaction rate constants at temperatures of 352, 362, 372 and 382 °C were calculated from the Arrhenius equation, in which the pre-exponential factor and the activation energy were obtained by fitting the calculated experimental reaction rate constant data as described above. In this process, the activation energies and the pre-exponential factors for all the individual sulphur compounds were also obtained. Since the data used here were obtained at different temperatures, the effective diffusion coefficient in Eq. (4) is automatically treated as a function of temperature.

Fig. 6 shows the catalyst effectiveness factors at different temperatures for DBT, 4-MDBT, 4,6-DMDBT and 2,4,8-TMDBT. In the range of temperature used, the variation of effectiveness factor with temperature is approximately linear. As expected, the effectiveness factors decreased with increasing temperature. This is because temperature has a greater effect on the intrinsic reaction rate constant than the intra-particle effective diffusion coefficient. The calculated effectiveness factors for each individual sulphur compound at different temperatures are listed in Table 2. For the 25 DBTs, the effectiveness factors ranged from 0.300 for 2,7-DMDBT to 0.822 for 4,6-DMDBT in the full-size catalyst, indicating that significant intra-particle diffusion resistance was present for all the sulphur compounds considered. The intra-particle diffusion effect was much less pronounced in the crushed catalyst particles, yet it was not completely eliminated. The effectiveness factors in the crushed catalyst particles exceeded 0.9 for most of the sulphur compounds in the entire temperature range, except for 2-MDBT, 3-MDBT, 2,7-DMDBT, 2,8-DMDBT and 3,7-DMDBT (above 0.8). DBTs with relatively higher HDS reactivities, such as DBT, 2- and 3-MDBT and 2,7-DMDBT, had lower effectiveness factors than DBTs with relatively lower HDS reactivities (4,6-DMDBT, 2,4,6-TMDBT, 3,4,6-TMDBT and 4-E-6-M-DBT).

This observation can be explained with Eq. (4) as follows. The differences in the molecular size among all the DBTs examined in this study were relatively small, and therefore the

Table 2

Catalyst effectiveness factors for total sulphur, total nitrogen and individual sulphur compounds

Sulphur compound	Effectiveness factor, full-size catalyst				Effectiveness factor, crushed catalyst			
	$T = 352\text{ }^{\circ}\text{C}$	$T = 362\text{ }^{\circ}\text{C}$	$T = 372\text{ }^{\circ}\text{C}$	$T = 382\text{ }^{\circ}\text{C}$	$T = 352\text{ }^{\circ}\text{C}$	$T = 362\text{ }^{\circ}\text{C}$	$T = 372\text{ }^{\circ}\text{C}$	$T = 382\text{ }^{\circ}\text{C}$
Total S	0.633	0.615	0.598	0.582	0.959	0.956	0.953	0.949
Total N	0.750	0.731	0.713	0.696	0.977	0.975	0.972	0.970
DBT	0.484	0.472	0.460	0.449	0.922	0.917	0.913	0.908
1-MDBT	0.524	0.494	0.466	0.440	0.934	0.925	0.915	0.904
2-MDBT	0.387				0.878			
3-MDBT	0.374				0.870			
4-MDBT	0.595	0.582	0.568	0.556	0.952	0.949	0.946	0.943
1,4-DMDBT	0.644	0.615	0.589	0.563	0.961	0.956	0.950	0.945
1,6-DMDBT	0.631	0.619	0.606	0.595	0.959	0.957	0.954	0.952
2,4-DMDBT	0.564	0.528	0.494	0.462	0.945	0.935	0.925	0.914
2,6-DMDBT	0.644	0.598	0.557	0.518	0.961	0.953	0.943	0.933
2,7-DMDBT	0.300				0.813			
2,8-DMDBT	0.390	0.515	0.489	0.464	0.880			
3,4-DMDBT	0.544	0.532	0.507	0.483	0.940	0.932	0.923	0.914
3,6-EDBT	0.559				0.943	0.936	0.929	0.921
3,7-DMDBT	0.364				0.865			
4,6-DMDBT	0.822	0.796	0.771	0.748	0.985	0.983	0.980	0.977
4-EDBT	0.696	0.629	0.570	0.516	0.970	0.959	0.946	0.932
1,3,7-TMDBT	0.588	0.572	0.556	0.541	0.950	0.947	0.943	0.939
1,4,6-TMDBT	0.689	0.675	0.663	0.651	0.969	0.967	0.965	0.963
1,4,7-TMDBT	0.731	0.699	0.670	0.642	0.975	0.970	0.966	0.961
2,4,6-TMDBT	0.734	0.717	0.700	0.684	0.975	0.973	0.970	0.968
2,4,7-TMDBT	0.539	0.487	0.439	0.397	0.938	0.922	0.904	0.884
2,4,8-TMDBT	0.502	0.481	0.460	0.441	0.928	0.920	0.913	0.905
3,4,6-TMDBT	0.780	0.766	0.752	0.739	0.981	0.979	0.978	0.976
3,4,7-TMDBT	0.710	0.678	0.647	0.619	0.972	0.967	0.962	0.957
4-E-6-M-DBT	0.758	0.716	0.676	0.640	0.978	0.973	0.967	0.961

differences in their intra-particle diffusivities (D_e) were also small. However, these DBTs had very different intrinsic kinetics rate constants ($k_{\text{intrinsic}}$) as observed in this study as well as in our previous studies [5,6]. DBTs with no or little steric hindrance effect by methyl/ethyl groups, such as DBT, 2- and 3-MDBT and 2,7- and 2,8-DMDBT, had much higher $k_{\text{intrinsic}}$ than those with strong steric hindrance effect, such as 4-MDBT, 4,6-DMDT, 2,4,6- and 3,4,6-TMDBT, and 4-E-6-M-DBT. Higher $k_{\text{intrinsic}}$ resulted in higher Thiele modulus and, therefore, lower catalyst effectiveness factors.

3.4. Implication

As discussed above, catalyst effectiveness factors for DBTs range from 0.3 to 0.8 in commercial hydrotreating catalysts, indicating a poor utilization of the catalyst intrinsic activity. This calls for HDS process innovations, including optimizing catalyst size, shape and operating conditions to maximize the catalyst performance. Furthermore, a completely new type of reactor might be a better solution to improve the catalyst utilization, such as monolith catalytic reactors. The small channels of the monolith catalysts provide void space for gas and liquid flow, while the channel walls, made of porous catalyst, allow the reactants to diffuse into the catalyst pores and react there [16,17]. The size and shape of the channels, and the channel wall thickness, can be independently optimized to get the maximum catalyst efficiency per unit volume of the reactor [18]. Both experimental and theoretical studies are much needed in this area to explore the application of monolith reactors to refining processes.

4. Concluding remarks

A comparative HDS study has been conducted in a pilot plant hydrotreater with a commercial hydrotreating catalyst using commercial-size extrudates and crushed particles under similar operating conditions. Experimental results showed that significant intra-particle diffusion limitations were present in the full-size commercial catalyst for all the DBTs investigated in this study. The corresponding catalyst effectiveness factors for these DBTs ranged between 0.300 and 0.822 in the temperature range studied. The intra-particle diffusion resistance was much less pronounced but still present in the crushed catalyst. The effectiveness factors for the crushed catalyst ranged from 0.813 to 0.985 in the same temperature range. As expected, the catalyst effectiveness factors decreased with

temperature. The DBTs with little or no steric hindrance effect had lower effectiveness factors (stronger intra-particle diffusion effects), whereas the DBTs with strong steric hindrance effect had higher effective factors (weaker intra-particle diffusion effects). Much improved efficiency of HDS could likely be achieved by increasing catalyst utilization, achievable through reconfiguration of the hydrotreater.

Acknowledgements

The authors are grateful to the following individuals for their help and support: Renata Szykarczuk and Dennis Carson for conducting the pilot plant experiments, Yevgenia Briker and Cecile Lay for sulphur speciation analysis, and Norm Sacuta for paper editing. Partial funding for NCUT has been provided by the Canadian Program for Energy Research and Development (PERD), the Alberta Research Council (ARC) and the Alberta Energy Research Institute (AERI).

References

- [1] C. Song, *Catal. Today* 86 (2003) 211.
- [2] F.L. Plantenga, E. Brevoord, S. Mayo, Y. Inoue, H. Tokumoto, *Oil Gas Eur. Mag.* 3 (2003) 37.
- [3] I.V. Babich, J.A. Moulijn, *Fuel* 82 (2003) 607.
- [4] R.E. Levy, A.S. Rappas, F.-M. Lee, V.P. Nero, S.J. DeCanio, *Hydro. Eng.* 7 (2002) 25.
- [5] J. Chen, Z. Ring, *Fuel* 83 (2004) 305.
- [6] J. Chen, M. Te, H. Yang, Z. Ring, *Petrol. Sci. Technol.* 21 (2003) 911.
- [7] V.R. Kumar, K.S. Balaraman, V.S.R. Rao, M.S. Ananth, *Petrol. Sci. Technol.* 19 (2001) 1029.
- [8] E. Lecrenay, K. Sakanishi, I. Mochida, *Catal. Today* 39 (1997) 13.
- [9] T. Kabe, K. Akamatsu, A. Ishihara, S. Otsuki, M. Godo, Q. Zhang, W. Qian, *Ind. Eng. Chem. Res.* 36 (1997) 5146.
- [10] V. Vanrysselberghe, G.F. Froment, *Ind. Eng. Chem. Res.* 37 (1998) 4231.
- [11] J. Chen, Z. Ring, Presentation at 2004 AIChE Spring Meeting, New Orleans, LA, USA, April 25–29, 2004, paper 115b.
- [12] Z. Ring, J. Chen, H. Yang, H. Du, Y. Briker, Proceedings of 7th International Conference on Refinery Processing (2004 AIChE Spring Meeting), New Orleans, LA, USA, April 25–29, 2004, pp. 355.
- [13] J. Chen, H. Yang, Z. Ring, *Catal. Today* 98 (2004) 227.
- [14] G.F. Froment, G.A. Depauw, V. Vanrysselberghe, *Ind. Eng. Chem. Res.* 33 (1994) 2975.
- [15] J. Ancheyta, M.J. Angeles, M.J. Macías, G. Marroquín, R. Morales, *Energy Fuels* 16 (2002) 189.
- [16] T.A. Nijhuis, M.T. Kreutzer, A.C.J. Romijn, F. Kapteijn, J.A. Moulijn, *Chem. Eng. Sci.* 56 (2001) 823.
- [17] W. Liu, *AIChE J.* 48 (2002) 1519.
- [18] S. Roy, A.K. Heibel, W. Liu, T. Boger, *Chem. Eng. Sci.* 59 (2004) 957.